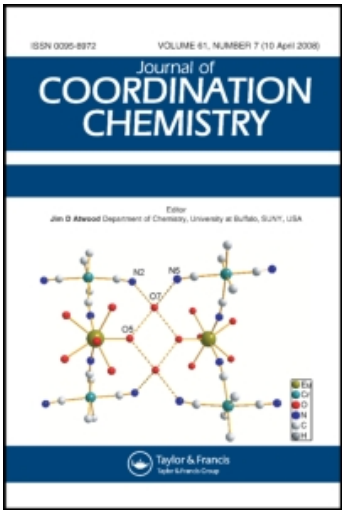

Journal of Coordination Chemistry
Publication details, including instructions for authors and subscription information:
http://www.informaworld.com/smpp/title~content=t713455674

Synthesis, spectral and antimicrobial studies of rare earth metal complexes with Schiff-base hydrazone containing quinoline moiety

Khlood S. Abou-Melha[a]; Hanan Faruk[a]
[a] Department of Chemistry, Education College for Girls, Scientific Departments, Assir, Abha, Saudi Arabia, KSA

To cite this Article Abou-Melha, Khlood S. and Faruk, Hanan(2008) 'Synthesis, spectral and antimicrobial studies of rare earth metal complexes with Schiff-base hydrazone containing quinoline moiety', Journal of Coordination Chemistry, 61: 12, 1862 — 1874
To link to this Article: DOI: 10.1080/00958970701768455
URL: http://dx.doi.org/10.1080/00958970701768455

Journal of Coordination Chemistry
Vol. 61, No. 12, 20 June 2008, 1862–1874

Taylor & Francis
Taylor & Francis Group

Synthesis, spectral and antimicrobial studies of rare earth metal complexes with Schiff-base hydrazone containing quinoline moiety

KHLOOD S. ABOU-MELHA* and HANAN FARUK

Department of Chemistry, Education College for Girls,
Scientific Departments, Assir, Abha, Saudi Arabia, KSA

(*Received 8 May 2007; in final form 18 July 2007*)

The synthesis and characterization of lanthanide(III) complexes with the Schiff-base hydrazone, *o*-hydroxyacetophenone-7-chloro-4-quinoline, (HL) are reported. The complexes were characterized by different physicochemical methods: mass spectrometry, ^{1}H NMR, ^{13}C NMR, and IR, UV-visible, molar conductance and magnetic studies. They have the stoichiometry $[Ln(L)_2(NO_3)] \cdot nH_2O$ where Ln = La(III), Pr(III), Nd(II), Sm(III), Eu(III) and $n = 1$–3. The spectra of the complexes were interpreted by comparison with the spectrum of the free ligand. The Schiff-base ligand and its metal complexes were tested against one stain Gram +ve bacteria (*Staphylococcus aureus*), Gram −ve bacteria (*Escherichia coli*), and Fungi (*Candida albicans*). The tested compounds exhibited high antimicrobial activities

Keywords: Schiff-base ligand; Metal complexes; Antimicrobial

1. Introduction

During the past two decades, considerable attention has been paid to the chemistry of the metal complexes of Schiff bases containing nitrogen and other donors [1–4] because of their stability, biological activity [5–11] and potential applications in fields such as oxidation catalysis [12], electrochemistry [13], etc. Coordination compounds of aroylhy-drazones have been reported to act as enzyme inhibitors and have useful pharmacological applications [6, 14]. Hydrazones derived from condensation of isonicotinic acid hydrazide (INH) with pyridine aldehydes have been found to show better antitubercular activity than INH [14].

The use of rare earth elements (REE) in agriculture to promote the growth of plants is well known [15–17]. Lanthanide complexes of a few compounds exhibit fungicidal and bactericidal activities including regulating the growth of plants [17–20]. It is known that chelation of metal ions with organic ligands acts synergistically to increase

*Corresponding author. Email: khold_melha@yahoo.com

Journal of Coordination Chemistry
ISSN 0095-8972 print/ISSN 1029-0389 online © 2008 Taylor & Francis
DOI: 10.1080/00958970701768455

its effect [21]. Metal complexes of some 3d elements of hydrazone derived from 4,7-dichloroquinoline have been previously reported [22].

In the present work, we report the synthesis, spectral, and antimicrobial studies of lanthanide(III) complexes of the Schiff-base hydrazone, *o*-hydroxyacetophenone-7-chloro-4-quinoline, (HL).

2. Experimental

2.1. *Materials*

Reagent grade chemicals were used without further purification. *o*-Hydroxyacetophenone, and 7-chloro-4-hydrazinoquinoline were either BDH or Merck products. Organic solvents used were reagent grade.

2.2. *Measurements*

The metal contents of the complexes were determined by complexometric titrations against EDTA. Carbon, hydrogen, and nitrogen analyses were carried out at the Micro Analytical Center, Cairo University, Giza, Egypt. Electronic spectra were recorded for a solution of HL in DMF, and for the metal complexes as Nujol Mulls on a Jasco UV-VIS spectrophotometer model V-550 UV-V1S. The IR spectra were recorded using KBr discs on a FT-IR 1650 Perkin-Elmer Spectrometer. ^{1}H NMR spectra were carried out in DMSO-d_6 at room temperature using TMS as internal standard on a Brucker 250 MHz spectrophotometer. Magnetic susceptibilities of the complexes were measured by the Gouy method at room temperature using a model MK1 Johnson Matthey Alpha products magnetic susceptibility balance. Molar conductivities in DMF (10^{-3} M) at room temperature (28°C) were measured using a model LBR, WTWD-812 Wilhelm Conductivity meter fitted with a model LTA100 cell. The TG-DTA measurements were carried out on a Shimadzu thermo gravimetric analyzer in dry nitrogen and a heating rate of 10°C min^{-1} using the TA-50 WS1 program. EI mass spectra were recorded on an MS 5988 Hewlett-Packard mass spectrometer. The sample was ionized by electron beam emitted from the filament, the generated ions being effectively introduced into the analyzer. EI mass spectra were obtained at ionizing energy values of 70 eV, ionization current of 60 mA and vacuum of 10^{-6} Torr. Lanthanide nitrates were prepared by dissolving the corresponding oxide (99.99%) in 50% HNO_3, followed by the evaporation of excess acid.

3. Synthesis

3.1. *Synthesis of the ligand, HL*

The ligand HL was prepared following the previously published method [22] by adding *o*-hydroxyacetophenone (1.5 g, 1.1 mmol, dissolved in 10 mL absolute ethanol) to 7-chloro-4-hydrazinoquinoline, (0.2 g, 1 mmol dissolved in 10 mL absolute ethanol).

The reaction mixture was stirred thoroughly and refluxed for 2 h, golden orange crystals precipitated which were filtered and washed with few drops of ethanol.

3.2. *Preparations of the metal complexes*

The ligand was first converted into its sodium salt by refluxing NaOH (2 mmol, 0.080 g) and HL (2 mmol, 0.622 g) in 20 mL methanol for 30 min. $Ln(NO_3)_3$ (1 mmol) dissolved in minimum methanol was added and further refluxed for 3 h. The solution was then concentrated to a small volume and the precipitate obtained was filtered, washed with water and ethanol, and air-dried. Yield: ~75%. The complexes were insoluble in water, slightly soluble in methanol and ethanol, and well soluble in DMSO.

4. Pharmacology

The *in vitro* evaluation of antimicrobial activity was performed according to the diffusion technique [23]. The purpose of the screening program is to provide antimicrobial activity and bacteriostatic and fungistatic efficiency of the investigated compounds. Bacteria including *Staphylococcus aureus* and *Escherichia coli* were grown in nutrient broth at 37°C for 24 h. *Candida albicans* and *Fusarium solani* were grown in malt broth at 28°C for 48 h.

The ligand/complexes were tested using the diffusion technique [23] on solid media. Sterile (5 mm) diameter sensitivity discs were impregnated with different conc. of the ligand/complex (50 μg or 100 μg mL^{-1}) in DMF. Discs of each tested compound were laid onto nutrient agar for bacteria or potato dextrose agar for fungi. Plates are surface spread with 0.2 mL of logarithmic phase bacteria or fungi cultures. A 0.5 mL spore suspension (10^8 spores mL^{-1}) for bacteria or for filamentous fungi was also spread onto potato dextrose agar plates. The plates were then incubated for 24 h at 37°C for bacteria and 28°C for 48 h for fungi. Additionally antibiotic discs for Terbinafin and Streptomycin are tested as positive control. The results were recorded by measuring the zones of growth inhibition surrounding the discs.

5. Results and discussion

5.1. *Schiff base*

The organic ligand, HL, (figure 1) was prepared by reacting *o*-hydroxyacetophenone with 7-chloro-4-hydrazinoquinoline in the molar ratio 1 : 1. Elemental analyses of the ligand gave the molecular formula given in table 1. The ^1H NMR spectrum of the ligand in deuterated DMSO-d_6 showed signals at δ 14.5 and 11.7 ppm for the proton of the phenolic OH and the NH groups, respectively [24, 25]. A signal is also observed at δ 2.4 ppm for the $-CH_3$ group [24, 25]. Addition of D_2O to the previous solution results in diminishing the signals due to the protons of phenolic OH.

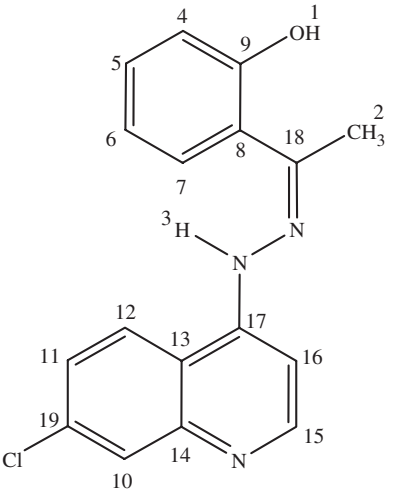

Figure 1. *o*-Hydroxyacetophenone-7-chloro-4-quinoline hydrazone, HL.

Table 1. Elemental analyses, yields, and melting points of HL and its metal complexes.

Compound (F.W.)	Yield (%)	Dec. P. (°C)	Elemental analysis, Found/(Calcd) %				
			C	H	N	Cl	M
HL	66	225[a]	65.85	5.12	13.12	11.26	–
$C_{17}H_{14}N_3OCl$ (311.5)			(65.49)	(4.49)	(13.48)	(11.40)	
$[La(L)_2(NO_3)] \cdot 2H_2O$	33	247[b]	47.12	3.32	11.22	8.53	16.54
$C_{34}H_{30}N_7O_7Cl_2La$ (858)			(47.55)	(3.50)	(11.42)	(8.28)	(16.20)
$[Pr(L)_2(NO_3)] \cdot H_2O$	25	230[b]	48.23	3.56	11.32	8.60	17.10
$C_{34}H_{28}N_7O_6Cl_2Pr$ (841)			(48.51)	(3.33)	(11.65)	(8.44)	(16.65)
$[Nd(L)_2(NO_3)] \cdot 3H_2O$	55	234[b]	46.54	3.82	12.52	8.47	16.34
$C_{34}H_{32}N_7O_8Cl_2Nd$ (881)			(46.31)	(3.63)	(12.71)	(8.06)	(16.35)
$[Sm(L)_2(NO_3)] \cdot 2H_2O$	47	235[b]	47.21	3.95	11.63	8.64	17.70
$C_{34}H_{30}N_7O_7Cl_2Sm$ (869)			(46.95)	(3.45)	(11.28)	(8.17)	(17.26)
$[Eu(L)_2(NO_3)] \cdot 2H_2O$	34	240[b]	47.34	3.22	11.76	8.61	17.22
$C_{34}H_{30}N_7O_7Cl_2Eu$ (871)			(46.84)	(3.44)	(11.25)	(8.15)	(17.45)

[a]Dec. P. – Decomposition point. [b]Melting point.

The Schiff-base ligand, HL could be a tetradentate ligand with coordination sites being quinoline-nitrogen, azomethine-nitrogen, imine-nitrogen and the phenolic-oxygen. A comparison of the IR spectra (table 2) of the ligands and their metal complexes imply that the Schiff base is a monobasic bidendate ligand with phenolic-oxygen, and azomethine-nitrogen, a ON ligand.

The IR spectrum of the ligand exhibits several absorptions, due to the quinoline moiety, the azomethine group, the imine group and the phenolic OH group, table 2. The mass spectrum of the ligand showed its molecular ion peak at m/z 311 which coincides with the formula weight. The base peak observed at $m/z = 178$ amu corresponded to $[C_9H_6N_2Cl]^+$. Metastable ion(s) are not observed [25, 26]. Figure 2 shows the mass fragmentation pattern of HL.

Table 2. Characteristic IR bands (cm^{-1}) of HL and its metal complexes.

Compound	ν(C=N)	ν(N–H)	ν(N–N)	ν(M–N)	ν(M–O)	ν(OH), phenolic	Other bands
$HL=C_{17}H_{14}N_3OCl$	1605 s, 1615 m	3214 m	1140 s	–	–	3530 m, br	1278 (δOH– phenolic)
$[La(L)_2(NO_3)]\cdot 2H_2O$	1570 s, 1580 m	3215 m	1136 s	420 w	540 m	–	3439 m, br lattice water
$[Pr(L)_2(NO_3)]\cdot H_2O$	1575 m, 1580 m	3218 s	1137 w	425 w	520 m	–	3440 m, br lattice water
$[Nd(L)_2(NO_3)]\cdot 3H_2O$	1565 m, 1570 m	3215 s	1140 w	430 w	525 m	–	3434 m, br lattice water
$[Sm(L)_2(NO_3)]\cdot 2H_2O$	1580 sh, 1585 m	3215 m	1125 w	410 w	515 m	–	3436 m, br lattice water
$[Eu(L)_2(NO_3)]\cdot 2H_2O$	1575 sh, 1580 m	3218 s	1136 s	445 w	520 w	–	3438 m, br lattice water

s: strong, w: weak, m: medium, br.: broad.

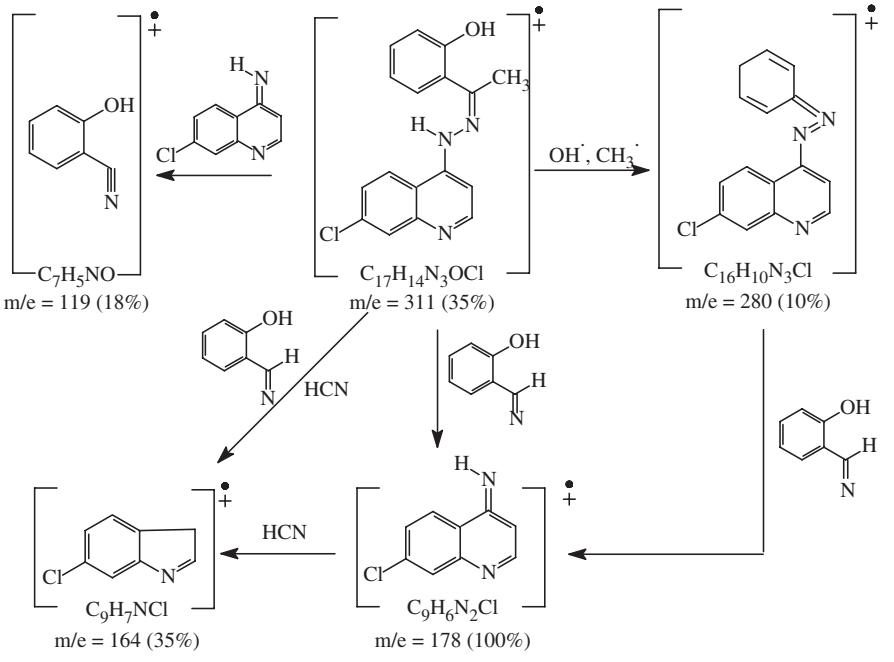

Figure 2. Mass fragmentation pattern of the ligand HL, the mass spectrum is recorded at 300°C and 70 eV.

5.2. *Metal complexes*

The compositions of the complexes of HL were confirmed by elemental analysis, DTA and TGA, and mass-spectral analysis. The binding mode of HL was further elucidated by IR and ^1H and ^{13}C NMR spectra of the complexes compared the free ligand. The complexes were insoluble in water, slightly soluble in methanol and ethanol, and well soluble in DMF and DMSO. The complexes are amorphous powders, stable at room temperature, not showing any decomposition on standing for several days. The molar conductivity values of the complexes in 10^{-3} M DMF are in the range

4.4–9.6 $Ohm^{-1}\,cm^2\,mol^{-1}$ indicating their nonelectrolytic nature [26, 27]. Similar results were reported [28].

5.2.1. Infrared spectra. In the ν(O–H) region, the spectra of the complexes show strong sharp bands between 3426–3530 cm^{-1} attributed to water. The most important IR assignments in the spectrum of the free ligand, as well as the bonding sites in the metal complexes, have been determined by a careful comparison of the spectrum of the ligand and its metal complexes in order to ascertain the ligand to metal ion bonding modes. The spectra of the complexes show that HL is a monobasic bidentate ligand, coordinating via the C=N azomethine and the phenolic OH group with displacement of a hydrogen atom from the latter. The changes in the spectra of the complexes are suggested by the following evidence.

The disappearance of the phenolic (OH) band and the absence of a broad band at 3530 cm^{-1} indicate deprotonation of the phenolic oxygen and cleavage of the hydrogen bond with involvement of the oxygen in bonding; the appearance of a new band at ca 520 cm^{-1} is assigned to the (Ln–O) vibration [24, 25]. A strong band at 1465 cm^{-1} assigned to ν(C–O) in the spectrum of the ligand shifts to lower frequency by ca 40 cm^{-1}, indicating participation of the phenolic oxygen in coordination, subsequent to deprotonation [14, 22, 29–30]. The bands observed in the spectrum of the ligand at 1605, 1615 cm^{-1} assigned for ν_s and ν_{as} of the C=N group are shifted in all spectra of the complexes to lower frequency and appear at ca 1570–1560 cm^{-1} indicating involvement of the N-atom of the azomethine in coordination. Moreover, the band due to the imine, NH, which appeared at 3214 cm^{-1} [24, 25] in the IR spectrum of the parent ligand remains unchanged in the IR spectrum of the complexes.

The bands observed at 1586–l740 assigned for ν(C=C) + ν(C=N) of the quinoline ring and at 577–462 and 478–700 due to in- and out-plane quinoline ring deformations, respectively, and the quinoline ring breathing, observed at 827–1013 cm^{-1} in the spectrum of the ligand remain unchanged in frequency and band intensity revealing noninvolvement of quinolinic-nitrogen in coordination with the metal. In all the IR spectra of the complexes, new bands with medium to weak intensities appear at 515–540 and 410–445 cm^{-1} in the complexes which are tentatively assigned to ν(M–O) and ν(M–N) modes, respectively [25, 29, 30].

For the nitrate group, applying the method described previously [31–35], the two strong absorptions at ~1500 and 1300 cm^{-1} are attributed to ν_4 and ν_1 modes for covalently bonded nitrate groups. This suggests that nitrate groups are coordinated and a separation of 15–25 cm^{-1} observed in the combination bands $(\nu_1) + (\nu_4)$ in the 1700–1800 cm^{-1} region indicates monodentate nitrate coordination. A similar result was reported by Agarwal [36].

In conclusion, the infrared spectral studies suggest monobasic bidentate nature of the ligands with ON coordination sites through phenolic OH, and azomethine groups.

5.2.2. ^1H and ^{13}C NMR spectra. The Ln(III) complexes and the ligand were further studied by ^1H and ^{13}C NMR spectra of the lanthanum complex as a representative complex of these series. The ^1H NMR spectrum showed disappearance of the signal due to the proton of the phenolic OH group which is attributed to its coordination to La^{3+}. The signal due to the NH proton remains at $\delta = 12.4$ ppm compared to that of the ligand at $\delta = 11.7$ ppm indicating the noninvolvement of the nitrogen atom of the imine

Table 3. ^{13}C NMR spectral data of the ligand and lanthanum complex.

Atom	$HL = C_{17}H_{14}N_3OCl$	$[La(L)_2(NO_3)] \cdot 2H_2O$
C2	20.1	20.5
C4	116	118
C5	132.5	133.0
C6	121.5	121.8
C7	130.6	130.6
C8	118.8	120.5
C9	161.1	165.3
C10	129.4	129.7
C11	127.3	128.1
C12	122.5	125.6
C13	119.7	120.8
C14	148.1	148.1
C15	151.3	153.1
C16	113.0	114.4
C17	149.5	150.5
C18	168.7	169.7
C19	134.9	135.1

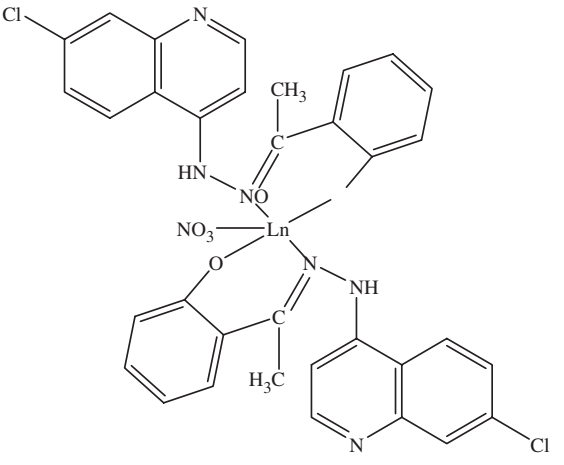

Figure 3. Suggested structure of the lanthanide complexes.

group in coordination. The signal due to the CH_3 remains unchanged to the parent ligand (at $\delta = 2.2$ ppm). Signals due to the aromatic ring showed fine structure as four separate signals at $\delta = 6.9$, 7.4, 7.6 and 8.2 ppm. Also, the spectrum showed additional signals due to coordinated H_2O [23, 24] at $\delta = 3.5$ ppm.

The chemical shifts of the protons vary in the lanthanide complexes, because of the shift properties of the lanthanide metals. Due to electron transfer from the phenolic-oxygen and azomethine-nitrogen atoms to Ln(III) ion, chemical shifts to lower ppm were observed for the neighboring C-9 and C-18 carbon atoms of the complex confirming coordination of the ligand through both deprotonated phenolic OH and azomethine-nitrogen atoms (table 3). The other carbon atoms were only slightly affected from the coordination of the metal. On the basis of the results thus obtained, it was suggested that the ligand is monobasic didentate in the Ln(III) complexes as shown in figure 3.

5.2.3. Mass spectra. The elemental analysis data of the Ln(III) complexes obtained are in agreement with the formula $[Ln(L)_2(NO_3)] \cdot nH_2O$, where Ln = La(III), Pr(III), Nd(II), Sm(III), Eu(III), $L = [C_{17}H_{13}N_3OCl^{1-}$ and $n = 1$–3. The suggested formulas were further confirmed by mass-spectral fragmentation analysis. Many lanthanides possess several isotopes and the MS peak patterns are therefore characteristic of the nature of the cation present. Neodymium and samarium have several isotopes and the peak pattern of the compound containing this metal is therefore much more complicated. The spectra (although with low intensity) showed isotopic patterns centered around m/z (%) 858 (8), 841 (5), 881 (8), 869 (5) and 871 (5) for La, Pr, Nd, Sm and Eu-complexes, respectively, corresponding to the mass weights of the complexes. The results thus obtained are in agreement with metal:ligand ratio, 1 : 2.

5.2.4. UV-visible spectra. The electronic spectrum of HL displays absorption bands at 35,842, and 33,333, cm^{-1} which are assigned to the π–π^* transitions within the aromatic and quinoline. The bands at 32,838 and 27,425 cm^{-1} are attributed to the n–π^* transition of the C=N (azomethine) and C=N (quinoline), respectively. Absorption bands at 26,178 and 25,178 cm^{-1} assigned for CT transitions, encroach on the visible region and give the ligand its color [24, 25]. The electronic spectra of the complexes are similar to the ligand except for a very slight shift towards lower frequency. A comparison of the transitions of the complexes with their corresponding aquo ions has been made (table 4). These data clearly indicate that the energy of f–f transitions in the complexes is slightly reduced from the corresponding aquo ions, due to covalent interaction of 4f orbitals with vacant ligand orbitals or increased nuclear shielding of f-orbitals due to slight L–M electron transfer [37]. The nephelauxetic ratio (β), bonding parameter ($b^{1/2}$), Sinha's covalency parameter (δ%), and angular covalency (η) for the Pr(III) and Nd(III) complexes have been calculated [38–40]. The Sinha parameter (δ) is taken as a measure of covalency and is given by

$$\delta(\%) = \frac{1 - \beta_{av}}{\beta_{av}} \times 100 \tag{1}$$

where β_{av} is the average value of the ratio of $\nu_{complex}/\nu_{aquo}$. The bonding parameter ($b^{1/2}$), the magnitude of which suggests the comparative involvement of the 4f orbitals in metal-ligand bonding, is related to the nephelauxetic ratio β and is given by the expression

$$b^{1/2} = \left[\frac{1 - \beta_{av}}{2}\right]^{1/2} \tag{2}$$

δ values are less than one whereas the remaining values are positive indicating the interaction between the metal salts and ligand is mainly electrostatic.

5.2.5. Thermal analyses. Thermal decomposition data of $[Pr(L)_2(NO_3)] \cdot H_2O$ as a representative example is presented in table 5. Analyses of thermogravimetric curves suggest that the complex contains one lattice water which is evident by loss in weight

Table 4. Electronic spectral data of the ligand and its Pr(III) and Nd(III) complexes.

Complex	$\pi \rightarrow \pi^*$, $n \rightarrow \pi^*$ and charge transfer transitions UV (cm^{-1})	Electronic transitions	λ_{max} of Ln^{+3} ion (aqo) (cm^{-1})	λ_{max} of complex (cm^{-1})	B	Other parameters
$HL=C_{17}H_{14}N_3OCl$	35,842, 33,333, 32,838, 27,425, 26,178, 25,178	–	–	–	–	–
$[Pr(L)_2(NO_3)] \cdot H_2O$[a]	35,742, 32,333, 32,732, 27,325, 26,178, 25,178	$^3H_4 — ^3P_2$	22,512	22,502	0.99955	
		$— ^3P_0$	20,716	20,678	0.99816	$\delta = 0.10511$
		$— ^1D_2$	16,854	16,840	0.99916	$b^{1/2} = 0.02291$
		$^4I_{9/2} — ^2G_{9/2}$	19,747	19,565	0.99078	
$[Nd(L)_2(NO_3)] \cdot 3H_2O$[b]	35,642, 32,333, 31,732, 27,325, 26,178, 25,178	$— ^4G_{5/2}$	17,253	17,182	0.99588	$\delta = 0.707\ 97$
		$— ^4F_{9/2}$	14,594	14,450	0.99013	$b^{1/2} = 0.0592$
		$— ^4F_{5/2}$	12,853	12,790	0.99509	$\eta = 0.08414$

[a] $\beta_{average} = 0.99895$, $\delta = 0.10511$, $b^{1/2} = 0.02291$ and $\eta = 0.03242$.
[b] $\beta_{average} = 0.99297$, $\delta = 0.70797$, $b^{1/2} = 0.0592$ and $\eta = 0.08414$.

Table 5. Thermal decomposition data for the Pr(III) complex.

Complex	Dec. stages.	Reaction	Peak temp. (°C) in DTG	Temp. range in DTG (°C)	Peak temp. (°C) in DTA
$[Pr(L)_2(NO_3)] \cdot H_2O$	I	$[Pr(L)_2(NO_3)] \cdot H_2O \rightarrow [Pr(L)_2(NO_3)] + H_2O$	125	95–150	120 (endo)
$C_{34}H_{28}N_7O_6Cl_2Pr$ (841)	II	$[Pr(L)_2(NO_3)] \rightarrow C_{32}H_{22}N_4Cl_2Pr + 2CH_3NO_3$	350	320–420	375 (exo)
	III	$C_{32}H_{22}N_4Cl_2Pr \rightarrow$ deligandation and formation of the metal oxide	760	680–770	760 (exo)

Dec. = Decomposition.

Table 6. Antimicrobial activity of HL and its metal complexes.

Compound	Microbial species			
	(a)	(b)	(c)	(d)
$HL = C_{17}H_{14}N_3OCl$	++	++	++	++
$[La(L)_2(NO_3)] \cdot 2H_2O$	+++	+++	++	+++
$[Pr(L)_2(NO_3)] \cdot H_2O$	++	++	++	+++
$[Nd(L)_2(NO_3)] \cdot 3H_2O$	+++	++	+++	+++
$[Sm(L)_2(NO_3)] \cdot 2H_2O$	++	++	++	+++
$[Eu(L)_2(NO_3)] \cdot 2H_2O$	++	+++	+++	+++
Terbinafin[a]	+++	++	+++	++++
Streptomycin[b]	++++	+++	+++	++

(a) *Staphylococcus aureus*, (b) *Escherichia coli*, (c) *Candida albicans*, (d) *Fusarium solani*. Inhibition zone diameter in nm (% inhibition): +, 8–10 (36–45%); ++, 10–16 (45–73%); +++, 16–19 (73–86); ++++, 19–22 (86–100%). Percent inhabitation values are relative to inhabitation zone (22 mm) with 100% inhabitation. $L = [C_{17}H_{13}N_3OCl]^-$.
[a]Standard antifungal and [b]antibacterial agents.

at ~120°C. The complex showed a second decomposition step at 180°C in which the complex loses two CH_3NO_3 molecules. There is no change up to ~400°C after which the rest of the organic ligand begins to decompose at ~550°C. Finally, at ~760°C, metal oxide is formed [41].

6. Antimicrobial activities

A number of authors [15–17] have investigated the biological and medicinal properties of rare earth complexes. The lanthanide complexes of a few selected compounds have exhibited fungicidal and bactericidal activities including regulating the growth of plants [17, 20].

The Schiff-base ligand, HL, and its lanthanide complexes reported here were evaluated for antimicrobial activity against one strain Gram +ve bacteria (*S. aureus*) (a), Gram −ve bacteria (*E. coli*) (b), fungus (*C. albicans*), (c) and fungus *Fusarium solani*, (d). The obtained antimicrobial activities are presented in table 6. The Schiff-base HL is biologically active, however its metal complexes showed remarkable antimicrobial activity as a result of chelation of metal with organic ligands synergistically increasing its effect [21].

The table shows that all metal complexes exhibit antimicrobial activity against one or more strain, enhanced compared with the parent Schiff base. Remarkable enhancement was found for the La(III) and Nd(III) complexes.

Chelation tends to make a ligand a more potent bactericidal agent. This increased activity upon chelation is attributed to the positive charge of the metal partially shared with donor atoms present on the ligands and there is electron delocalization over the whole chelate ring. This, in turn, increases the lipophilic character of the metal chelate and favors its permeation through the lipid layers of the bacterial membranes. Generally, it is suggested that the chelated complexes deactivate various cellular enzymes, which play a vital role in various metabolic pathways of these microorganisms. Other factors such as solubility, conductivity and dipole moment, affected by the

presence of metal ions, may also increase the biological activity of the metal complexes compared to the ligand.

7. Conclusion

The results of this investigation support the suggested structures of the lanthanide metal complexes. The Schiff-base ligand is monobasic bidentate with ON coordination sites. The metal complexes enhanced the antimicrobial activity in compare with the free ligand.

References

[1] S.S. Djebbar, B.O. Benali, J.P. Deloume. *Polyhedron*, **16**, 2175 (1997).
[2] S. Yamada, *Coord. Chem. Rev*., **190–192**, 537 (1999).
[3] L. He, S.H. Gou, Q.F. Shi, M. Qian, C. Duan. *J. Chem. Crystallogr*., **29**, 207 (1999).
[4] J.C. Wu, N. Tang, W.S. Liu, M.Y. Tan, A.S.C. Chan. *Chin. Chem. Lett*., **12**, 757 (2001).
[5] C.M. Liu, R.G. Xiong, X.Z. You, Y.J. Liu, K.K. Cheung. *Polyhedron*, **15**, 4564 (1996).
[6] L. Savanini, L. Chiasserini, A.C. Gaeta, C. Pellerano. *Bioorg. Med. Chem*., **10**, 2193 (2002).
[7] O. Ei-ichiro. *Bioinorganic Chemistry*, Allyn and Bacon, Boston (1977).
[8] R. Alberlini, S. Pinelli, P. Lunghi. *Inorg. Chim. Acta*, **286**, 134 (1999).
[9] H. Elo, P. Lumme. *Inorg. Chim. Acta*, **136**(3), 149 (1987).
[10] H. Elo, I. Sunila, P. Lumme. *Inorg. Chim. Acta*, **136**(1), 61 (1987).
[11] M.A. Ali, M.H. Kabir, M. Nazimuddin, S.M.H. Majumder, M.T.H. Tarafder, M. Akhair. *Indian J. Chem*., **27A**, 1064 (1988).
[12] S.S. Djebbar, B.O. Benali, J.P. Deloume. *Transit. Metal. Chem*., **23**, 443 (1998).
[13] Y.J. Hamada. *Trans. Electron Devices*, **44**, 1208 (1997).
[14] R.K. Agarwal, L. Singh, D.K. Sharma, R. Singh. *Turk J. Chem*., **29** (2005).
[15] H. Fashui. *Biological Trace Element Research*, **87**, 191 (2002).
[16] W. Huo, F. Jian, S. Zhengzhi. *Biological Trace Element Research*, **64**, 27 (1998).
[17] S.S. Kukalenko, B.A. Bovykin, S.I. Shestakova. *Russian Chemical Reviews*, **54**(7), 676 (1985).
[18] J. Huang, Y. Yang, C. Yuan. *Ziran Kexueban*, **28**(3), 259 (1998).
[19] A. Botterher, T. Takeuchi, K.I. Meade, H.B. Gray, D. Cwikel, M. Kapon, Z. Don. *Inorg. Chem*., **36** 2498 (1997).
[20] Z. Li. *Huaxue Tong Bao*, **1**, 21 (1994).
[21] F. Cavanagh. *Analytical Microbiology*, Academic Press, New York, NY (1963).
[22] M. El-Behery, H. El-Twigry. *Spectrochim. Acta Part A: Mol. Biomol. Spectrosc*., **66**(1), 28 (2007).
[23] J.P. Anhalt, J.A. Washington. *Laboratory Procedures in Clinical Microbiology*, 2nd Edn, p. 281, Springer-Verlag, New York (1985).
[24] D.H. Williams, I. Fleming. *Spectroscopic Methods in Organic Chemistry*, p. 94, McGraw-Hill, New York (1966).
[25] R.M. Silverstein, G.C. Bassler, T.C. Morrill. *Spectrometric Identification of Organic Compounds*, John Wiley & Sons, New York (1991).
[26] S.B. Padhy'e, G.B. Kauffman. *Coord. Chem. Rev*., **63**, 127 (1985).
[27] W.J. Geary. *Coord Chem. Rev*., **7**, 81 (1971).
[28] K.B. Gudas, R.V. Shenoy, R.S. Vadavi, M.S. Patil, S.A. Patil, R.R. Hanchinal, S.A. Desai, H. Lohithaswa. *Bioinorg. Chem. Appl*., **2006**, 1 (2006).
[29] J. Selbin. *Chem. Rev*., **65**, 153 (1965).
[30] A.Z. El-Sonbati, A.A. El-Bindary. *Polish J. Chem*., **74**, 621 (2000).
[31] N.M. Karayannis, C.M. Mikulski, L.L. Pytlewski, M.M. Labes. *Inorg. Chem*., **13**, 1146 (1974).
[32] C.C. Addison, N. Logan, S.C. Wallwork, C.D. Garner. *Rev. Chem. Soc*., **25**(2), 289 (1971).
[33] R.E. Heter, W.E.L. Grossman. *Inorg. Chem*., **5**, 1308 (1966).
[34] J.R. Ferraro. *J. Mol. Spectrosc*., **4**, 99 (1960).
[35] G.S. Devi, P. Indrasenan. *Inorg. Chim. Acta*, **133**, 157 (1987).
[36] R.K. Agarwal, D. Sharma, L. Singh, H. Agrawal. *Bioinorg. Chem. Appl*., **2006**, 1 (2006).
[37] C.K. Jorgenson. *Acta Chem. Scandinavica*, **16**, 793 (1962).

[38] D.E. Henrie, G.R. Choppin. *J. Chem. Phy.*, **49**(2), 477 (1968).
[39] S.P. Sinha. *Spectrochim. Acta*, **22**, 1 (1966).
[40] C.K. Jorgenson. The Nephelauxetic Series. In *Progress in Inorganic Chemistry*, F.A. Cotton (Ed.), p. 4, Interscience Publishers, Division of John Wiley, New York, NY (1962).
[41] R.K. Agarwal. *Bioinorg. Chem. Appl.*, **3**, 271 (2006).